Article

Inhibitory Effect of Lychee Seed Saponins on Apoptosis Induced by Aβ25-35 through Regulation of the Apoptotic and *NF-κB* Pathways in PC12 Cells

Xiuling Wang [1,†], Hong Zhang [1,†], Jian Liu [1], Rong Chen [2,3], Yong Tang [1,4], Haixia Chen [1], Li Gu [1], Mao Li [1], Shousong Cao [1], Dalian Qin [1,*] and Jianming Wu [1,*]

[1] Department of Pharmacology, School of Pharmacy, Southwest Medical University, Luzhou 646000, China; wangxiulingbest@gmail.com (X.W.); m18989131787_1@163.com (H.Z.); belkn@sohu.com (J.L.); tangy1989@yeah.net (Y.T.); dna0805001@163.com (H.C.); tristan19810102@icloud.com (L.G.); batilimao@163.com (M.L.); shousongc@gmail.com (S.C.)
[2] Department of Human Anatomy, School of Preclinical Medicine, Southwest Medical University, Luzhou 646000, China; 13558927205@163com
[3] Department of Human Anatomy, School of Preclinical Medicine, Sichuan Vocational College of Health and Rehabilitation, Zigong 643000, China
[4] Pharmacy Intravenous Admixture Services, Affiliated Hospital of Traditional Chinese Medicine, Southwest Medical University, Luzhou 646000, China
[*] Correspondence: dalianqin@swmu.edu.cn (D.Q.); jianmingwu@swmu.edu.cn (J.W.);
Tel./Fax: +86-830-3162-291 (D.Q.); +86-830-3161-506 (J.W.)
[†] These authors contributed equally to this work.

Abstract: Neuronal apoptosis plays a critical role in the pathogenesis of Alzheimer's disease (AD). Previous studies have shown that lychee seed saponins (LSS), isolated and extracted from traditional Chinese medicine lychee seeds, possess many beneficial activities including anti-oxidation, anti-diabetes, anti-AD, etc. In the present study, we established an in vitro neuronal apoptotic model of PC12 cells induced by Aβ25-35 and studied the effect of LSS on apoptosis by the methods of Hoechst 33342/propidium iodide (PI) fluorescence double staining, Annexin V/PI double staining, and terminal deoxynucleotidyl transferase (TdT)-mediated dUTP nick-end labeling (TUNEL). We also investigated the effects of LSS on mitochondria membrane potential, the expressions of Bcl-2 and Bax proteins, and the mRNA expression and the nuclear translocation of *NF-κBp65* in PC12 cells. The results showed that LSS markedly inhibited apoptosis, improved the mitochondria membrane potentials, upregulated the expression of Bcl-2 protein, downregulated the expression of Bax protein, and decreased the mRNA expression and nuclear translocation of *NF-κBp65* in PC12 cells. The study demonstrated that LSS significantly inhibited apoptosis induced by Aβ25-35 via regulation of the apoptotic and *NF-κB* pathways in PC12 cells. Therefore, LSS has the potential to be developed as a novel agent or nutrient supplement for the prevention and/or treatment of AD.

Keywords: Alzheimer's disease; lychee seed saponins; Aβ25-35; PC12 cells; apoptosis; *NF-κB*

1. Introduction

Alzheimer's disease (AD) is a common progressive neurodegenerative disorder that is characterized by the abnormal deposition of senile plaques (SPs) and neurofibrillary tangles (NFTs) owing to formations of amyloid-β protein (Aβ) and hyperphosphorylation of Tau protein in the brain [1]. A recent study has shown that apoptosis played a key role in the pathology of AD and the apoptotic ratio was obviously increased in the neurons of hippocampus of AD rats compared to those of normal rats [2]. Furthermore, excessive apoptosis of neurons was closely related to neuronal loss in

the brains of AD rats [3,4]. Accumulating evidence suggests that the key pathological cause of AD is the neuronal injury and loss caused by neuronal apoptosis, although the accurate mechanism is still unknown.

Apoptosis is a biological process in which a sensitive cell proceeds towards programmed death upon receiving certainly stimuli. Neuronal apoptosis is influenced by multiple stimuli, such as activation of relevant enzymes [5], reactive oxygen species (ROS) [6], mitochondrial permeability transition [7], tumor necrosis factor-α (TNF-α) [8], Bcl-2, Bax, caspases [9], and so on. Aβ, as a hallmark in the pathogenesis of AD, can inhibit phosphatidylinositol 3 kinase (PI3K)/Akt to increase the expression of pro-apoptosis genes such as Bcl-2-associated death promoter (*BAD*), glycogen synthase kinase 3β (*GSK-3β*), and nuclear factor *(NF)-κB*, and lead to neuronal apoptosis [10,11]. Furthermore, the mitochondria, as the major site of adenosine triphosphate (ATP) generation, actively participated in the integration and implementation of different stimuli related to apoptosis [12]. In addition, distorted expressions of apoptosis-related proteins, including *Bak*, *Bad*, *Bax*, *Bcl-2*, *p53*, *Par-4*, and *Fas*, as well as the activation of caspases, have also been implicated in the pathogenesis of AD [13,14].

As a famous traditional Chinese medicine, lychee seed (Lizhi He in Chinese) has been recorded in the *Compendium of Materia Medica* (*Bencao Gangmu*) and exhibits many beneficial effects including anti-tumor [15], anti-oxidation [16], anti-virus [17,18], preventing liver injury [19], improving insulin resistance (IR) and sensitivity [20,21], and other pharmacological effects. Previous studies have shown that the chemical constituents of lychee seed are mainly saponins, organic acids, fatty acids, amino acids, sugars, and flavonoids [15]. Recently, studies have reported that the saponins from gypenoside, ginsenoside, and senegenin possess the effect of neuroprotection [22,23]. Our preliminary studies have shown that lychee seed saponins (LSS) significantly relieved the cognitive dysfunction in a rat model of type 2 diabetes, improving IR and inhibiting NF-κB-mediated apoptosis. Additionally, we found that LSS obviously decreased the formation of Aβ, tau protein, and advanced glycosylation end products (AGEs), as well as the release of mitochondrial cytochrome C, to execute its anti-apoptosis effect in the brains of AD rats [24]. In the present study, we investigated the anti-apoptotic effect of LSS by Hoechst 33342/propidium iodide (PI) fluorescence double staining, AnnexinV/PI double staining, and terminal dexynucleotidyl transferase (TdT)-mediated dUTP nick-end labeling (TUNEL) methods, mitochondria membrane potentials by Rhodamine 123 staining, the expressions of Bcl-2 and Bax proteins by Western blotting, and the mRNA expression and nuclear translocation of *NF-κBp65* by reverse transcription polymerase chain reaction (RT-PCR) or immunofluorescence analysis, respectively, in rat adrenal pheochromocytoma 12 (PC12) cells.

2. Materials and Methods

2.1. General Information

Aβ_{25-35} (Lot: Y-0044) was purchased from BIOSS Biotech Limited Company (Beijing, China). The Hoechst 33342/PI apoptotic assay kit was purchased from Sigma-Aldrich (St. Louis, MO, USA). The TUNEL apoptosis detection kit was purchased from BOSTER Biotech Limited Company (Wuhan, Hubei, China). The Annexin V-FITC/PI apoptotic detection kit was purchased from KeyGEN Biotech Corp., Ltd. (Nanjing, China). Rhodamine 123 was purchased from Yansheng biochemical reagent Co., Ltd. (Shanghai, China). The RT-PCR kit was purchased from TransGen Biotech Limited Company (Beijing, China). 4',6-diamidino-2-phenylindole dihydrochloride (DAPI) was purchased from Sigma-Aldrich (Milan, Italy). Anti-NF-κBp65 antibody was purchased from Invitrogen (Carlsbad, CA, USA). The CO_2 incubator and ultra-low temperature freezer were purchased from SANYO Electric Co., Ltd. (Moriguchi, Japan). The laser scanning confocal microscope was purchased from Leica DMIRB (Rueil Malmaison, France). The flow cytometer was purchased from Becton-Dickinson Labware (Franklin Lakes, NJ, USA). The gel imaging and analysis system ChemiDocXRS were purchased from Bio-Rad Laboratories, Inc. (Berkeley, CA, USA). The TC-512PCR amplification instrument was purchased from TECHNE (London, UK).

2.2. Cell Culture

PC12 cells were purchased from China Center for Type Culture Collection (CCTCC, Wuhan, Hubei, China). The cells were cultured in Dulbecco's modified Eagle's medium (DMEM) supplemented with 5% fetal bovine serum, 10% horse serum, penicillin (100 U/mL), and streptomycin (100 μg/mL) in a CO_2 incubator (5% CO_2, 37 °C) and renewed with new medium every 3–5 days. PC12 cell is a nervous-like cell derived from rat adrenal medulla pheochromocytoma and is a widely used cell line for the study of the nervous system in vitro [25].

2.3. Collection, Isolation, and Extraction of LSS

Lychee seed was purchased from the market in Luzhou (Luzhou, Sichuan, China) and authenticated by Professor Can Tang (Department of Chinese Materia Medica, School of Pharmacy, Southwest Medical University, Luzhou, Sichuan, China). One thousand grams of dried lychee seeds were ground and soaked in 1000 mL 70% ethanol overnight and extracted by percolation with 8000 mL 70% ethanol at a speed of 5 mL/min/kg. The solvents were evaporated under a vacuum and diluted to 5000 mL with distilled water and absorbed by D101 macroporous resins at speed of 6 mL/min. Finally, LSS was collected by elution with 800 mL 70% ethanol and concentrated to dryness by a rotary vacuum evaporator to yield 31.75 g of dried extract.

2.4. Establishment of an Apoptotic Cell Model of PC12 Cells Induced by Aβ25-35 and Drug Treatment In Vitro

First, PC12 cells were seeded at a density of 1.0×10^5 cells/well on six-well plates (2.0 mL). After being cultured for 24 h, the culture medium was replaced with a serum-free DMEM medium. Next, the cells were treated with different concentrations (0.95, 1.90, 3.80, and 7.60 mg/L) of LSS for 1 h; serum-free DMEM medium was used as control. Then the cells were placed in a CO_2 incubator and exposed to 20 μmol/L Aβ$_{25\text{-}35}$ for 12 h to establish the cell model of AD. All experiments were performed in triplicate.

2.5. Apoptotic Analysis of PC12 Cells by Hoechst 33342/PI Fluorescence Double Staining

Apoptotic assay was processed by Hoechst 33342/PI fluorescence double staining as described previously [26]. Briefly, PC12 cells were treated with different concentrations of LSS (0.95, 1.90, 3.80, and 7.60 mg/L) or medium as control, then 10 μL (100 mg/L) Hoechst 33342 and 5 μL (1 mg/L) PI were added to the culture medium for 15 min at 37 °C, then washed with PBS and made cell resuspensions. The nuclear morphological changes of apoptotic cells were observed under fluorescence microscope and the percentage of apoptotic cells was calculated according to the ratio of apoptotic cells to total cells.

2.6. Apoptotic Analysis of PC12 Cell by Annexin V/PI Double Staining

To confirm early apoptotic cells, flow cytometer were used through FITC-conjugated Annexin V and PI double staining as described previously [27]. PC12 cells were treated with different concentrations of LSS (0.95, 1.90, 3.80, and 7.60 mg/L) or medium as control and harvested with 0.25% trypsin, washed twice with PBS, resuspended in buffer and incubated with 5 μL AnnexinV-FITC and 5 μL PI for 15 min in the dark at 37 °C. Then the specific fluorescence of 12,000 cells was observed on a FACSCalibur (BD) system within 1 h. Data were analyzed according to the apoptotic ratio.

2.7. Apoptotic Analysis of PC12 Cells by TUNEL

The apoptotic studies were also carried out with TUNEL analyses as previous described [28]. PC12 cells were treated with different concentrations of LSS (0.95, 1.90, 3.80, and 7.60 mg/L) or medium as control and evaluated by TUNEL immunohistochemical assay according to the manufacturer's instruction. The apoptotic cells were showed brown colors in the nuclei of cells. The apoptotic ratio was calculated as the percentage of apoptotic cells among 100 cells by GD-10.0 image analysis system.

2.8. Mitochondrial Membrane Potential Examination in PC12 Cells

Rhodamine 123 was used as a probe to detect the changes of mitochondria membrane potentials ($\Delta\Psi$mt). Briefly, PC12 cells were washed twice with PBS and incubated with Rhodamine 123 at the concentration 1 µmol/L for 30 min at 37 °C in a CO_2 incubator. After washing twice with PBS, the cells were observed under a fluorescence microscope and images were recorded.

2.9. Western Blotting Analysis of the Protein Expressions of Bcl-2 and Bax in PC12 Cells

PC12 cells were seeded at a density of 1.0×10^5 cells/well on six-well plates (2.0 mL), after being cultured for 24 h, the culture medium was replaced with serum-free DMEM medium. Then, the cells were randomly divided into six groups, rinsed with a serum-free DMEM medium, and treated with serum-free medium (vehicle as control in two groups) or LSS (0.95, 1.90, 3.80, and 7.60 mg/L) for 1 h. Next, the cells in one control group and four groups of LSS were exposed to 20 µmol/L A$\beta_{25\text{-}35}$ and another control group was treated with a medium for 13 h without A$\beta_{25\text{-}35}$.

After being cultured for 12 h, the culture medium was withdrawn and the cells were washed with cold PBS for harvest. The cell pellets were disrupted in a cell lysis buffer, 0.5% NP-40, 50 mmol/L Tris-HCl, 120 mmol/L NaCl, 1 mmol/L EDTA, 0.1 mmol/L Na$_3$VO$_4$, 1 mmol/L NaF, 1 mmol/L PMSF, and 1 µg/mL leupeptin, pH 7.5), then the lysates were centrifuged at $9600 \times g$ for 15 min at 4 °C. The protein concentrations were determined using the bicinchoninic acid (BCA) method, after which equal amounts of protein (30 µg) were electrophoresed on 10% density of SDS-acrylamide gels. Following electrophoresis, the proteins were transferred from the gel to a nitrocellulose membrane using an electric transfer system. Non-specific binding was blocked with 5% skim milk in tris-buffered saline with tween (TBST) buffer, 5 mmol/L Tris-HCl, 136 mmol/L NaCl, and 0.1% Tween-20, pH 7.6) for 1 h. The blots were incubated with antibodies against Bcl-2 (1:1000), Bax (1:1000) or β-actin (1:800) overnight at 4 °C and were washed three times with $1\times$ TBST. Then, the blots were incubated for 1 h at room temperature with a 1:1000 dilution of horseradish peroxidase-labeled anti-rabbit or anti-mouse IgG and washed three times with $1\times$ TBST, the membranes were developed by incubation within the ECL Western detection reagents. The specific protein bands were visualized and analyzed with a ChemiDoc image analyzer (Bio-Rad, Hercules, CA, USA).

2.10. RNA Isolation and Analysis of NF-κBp65 mRNA Expression in PC12 Cells by RT-PCR

Total RNA from PC12 cells was extracted using TRIzol reagent. The purity and concentration of mRNA were determined by sepharose gel and UV spectrophotometer, respectively. cDNA was synthesized through the reverse transcription of 1 µg mRNA using Taq PCR Master Mix. The primer sequences for NF-κBp65 and glyceraldehyde-3-phosphate dehydrogenase (GAPDH) were as follows: rat NF-κBp65 5′-ACCAAAGACCCACCTCACC-3′ (forward) and 5′-CGCATTC AAGTCATAGTCCC-3′ (reverse); rat GAPDH 5′-CCTCAAGATTGTCAGCAAT-3′ (forward) and 5′-CCATCCACAGTCTTCTGAGT-3′ (reverse), respectively. The reaction of PCR was conducted according to the manufacturer's protocol. The products of PCR underwent 2% agarose gel electrophoresis with a weight marker of DL500 DNA molecular. Gel imaging and analysis system were conducted for examination and quantitative analyses. GAPDH was used as the control.

2.11. Nuclear Translocation of NF-κBp65 in PC12 Cells by Immunofluorescence Analysis

Nuclear translocation of NF-κBp65 was studied by immunofluorescence analysis. PC12 cells were fixed in 4% paraformaldehyde for 30 min at 4 °C, then washed with 0.1% PBS and incubated with the primary antibody (1:50) overnight at 4 °C. The cells were washed with 0.1% PBS and incubated with anti-NF-κBp65 antibody (1:400) for 1 h and stained with 4′, 6-diamidino-2-phenylindole dihydrochloride (DAPI). The images were recorded and assessed under fluorescence microscopy.

2.12. Statistical Analysis

All data are expressed as mean $\pm$ standard deviation (SD). Statistical differences of the data among the means of two or more groups were analyzed by one-way univariate analysis of variance (ANOVA). A difference at $p < 0.05$ was considered to be statistically significant (marked as *). The higher significance level was set at $p < 0.01$ (marked as **).

3. Results

3.1. Effects of LSS on the Aβ_{25-35}-Induced Apoptosis in PC12 Cells by Hoechst 33342/PI Fluorescence Double Staining, Annexin V/PI Double Staining, and TUNEL Analyses

The key pathogenesis of AD is the neuronal loss caused by apoptosis. Therefore, we studied the effect of LSS on apoptosis induced by Aβ_{25-35} in PC12 cells through Hoechst 33342/PI double staining under a fluorescence microscope. The representative morphological pictures of PC12 cells and the cell apoptotic ratio are illustrated in Figure 1. The picture in Figure 1(Aa) shows the characteristic preserved normal features of PC12 cells in the control cells without Aβ_{25-35} treatment, which the nuclei of cells appear blue fluorescence. However, higher levels of apoptotic cells with condensation of nuclear chromatin and fragmentation were detected in the cells treated with Aβ_{25-35} (20 µmol/L) for 12 h (Figure 1(Ab)). Interestingly, the numbers of apoptotic cells were obviously decreased after LSS (0.95–7.60 mg/L) treatment (Figure 1(Ac–f)). The summarized results of the apoptotic ratio of cells are shown in Figure 1B and indicate that Aβ_{25-35} treatment significantly increased apoptosis compared to control cells treated with vehicle ($p < 0.01$), but LSS significantly inhibited Aβ_{25-35}-induced apoptosis compared to vehicle treatment ($p < 0.01$) in PC12 cells.

Next, we investigated the effect of LSS on apoptosis induced by Aβ_{25-35} in PC12 cells with Annexin V/PI double staining by flow cytometric analysis and the results are shown in Figure 2. The data showed that Aβ_{25-35} (20 µmol/L) treatment for 12 h markedly increased apoptosis in PC12 cells to 21.89% $\pm$ 1.01% ($p < 0.01$) compared to 0.78% $\pm$ 0.07% in control cells treated with vehicle (Figure 2(Aa,b)). However, LSS treatments (0.95–7.60 mg/L) significantly decreased apoptotic cells ($p < 0.01$) in PC12 cells exposed to Aβ_{25-35} (20 µmol/L) to 11.59% $\pm$ 0.81%, 5.41% $\pm$ 0.43%, 3.20% $\pm$ 0.37%, and 1.81% $\pm$ 0.19%, respectively (Figure 2(Ac–f)). The summarized results also clearly demonstrated that LSS effectively inhibited apoptosis in a concentration-dependent manner in PC12 cells with Annexin V/PI staining by flow cytometric analysis (Figure 2B).

Finally, we further studied the apoptosis of PC12 cells by TUNEL immunohistochemical assay. The representative photomicrographs are shown in Figure 3, a few spontaneous apoptotic cells are clearly observed, with brown appearance in the control cells treated with a vehicle (Figure 3(Aa)). Higher levels of apoptosis were detected in the cells treated with 20 µmol/L Aβ_{25-35} (Figure 3(Ab)), and the apoptotic ratio obviously increased compared to that of the control cells ($p < 0.01$). However, the numbers of apoptotic cells were significantly decreased ($p < 0.01$) after LSS treatment (Figure 3Ac–f) compared to after vehicle treatment. The summarized results are illustrated in Figure 3B and the data also indicate that LSS can markedly inhibit the apoptosis induced by Aβ_{25-35} in PC12 cells. The results are consistent with those of the Hoechst33342/PI fluorescence double staining and AnnexinV/PI double staining methods.
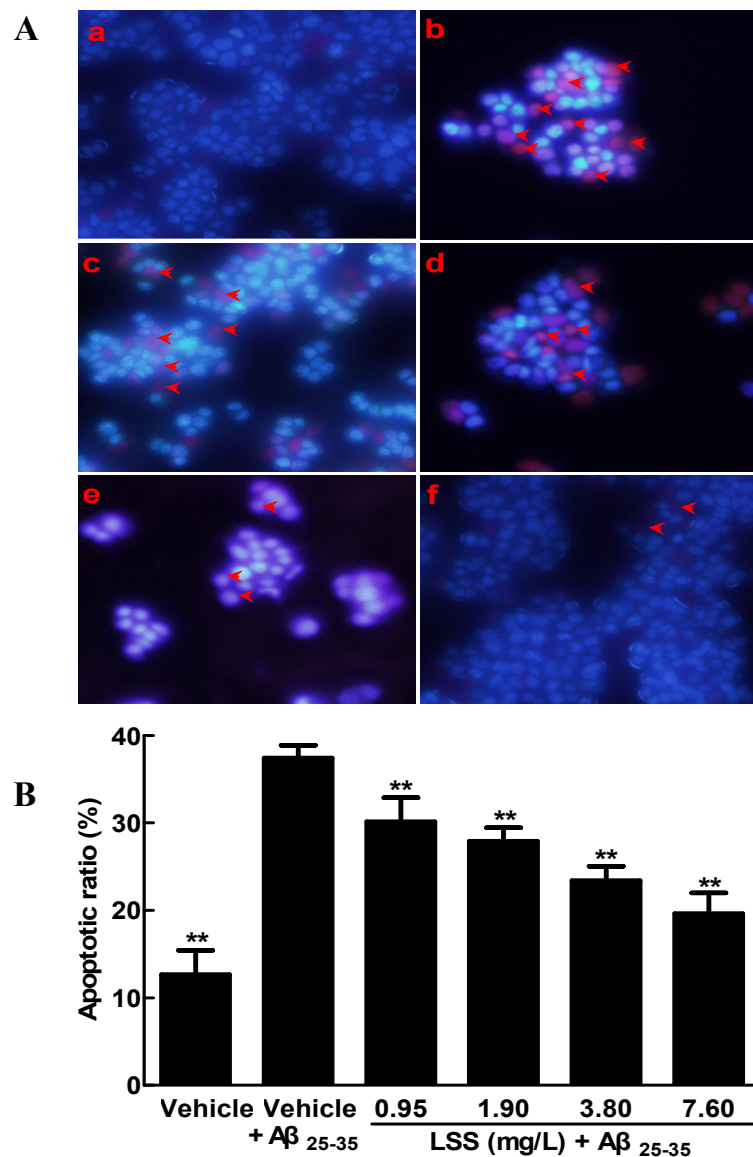
Figure 1. Effect of LSS on apoptosis induced by $A\beta_{25-35}$ (20 μmol/L) in PC12 cells with Hoechst 33342/PI staining under fluorescence microscope (400×). (**A**) Representative pictures of PC12 cells treated with or without LSS; (**Aa**) cells were treated with medium for 13 h without $A\beta_{25-35}$; (**Ab**) cells were treated with medium for 1 h and followed by $A\beta_{25-35}$ for 12 h; (**Ac**) cells were treated with LSS 0.95 mg/L for 1 h and followed by $A\beta_{25-35}$ for 12 h; (**Ad**) cells were treated with LSS 1.90 mg/L for 1 h and followed by $A\beta_{25-35}$ for 12 h; (**Ae**) cells were treated with LSS 3.80 mg/L for 1 h and followed by $A\beta_{25-35}$ for 12 h; (**Af**) cells were treated with LSS 7.60 mg/L for 1 h and followed by $A\beta_{25-35}$ for 12 h. The red arrows indicate apoptotic cells; (**B**) Summarized results of apoptotic ratio. The results are representative of at least three independent experiments run in triplicate and expressed as mean $\pm$ SD. ** $p < 0.01$ vs. cells treated with vehicle and $A\beta_{25-35}$.
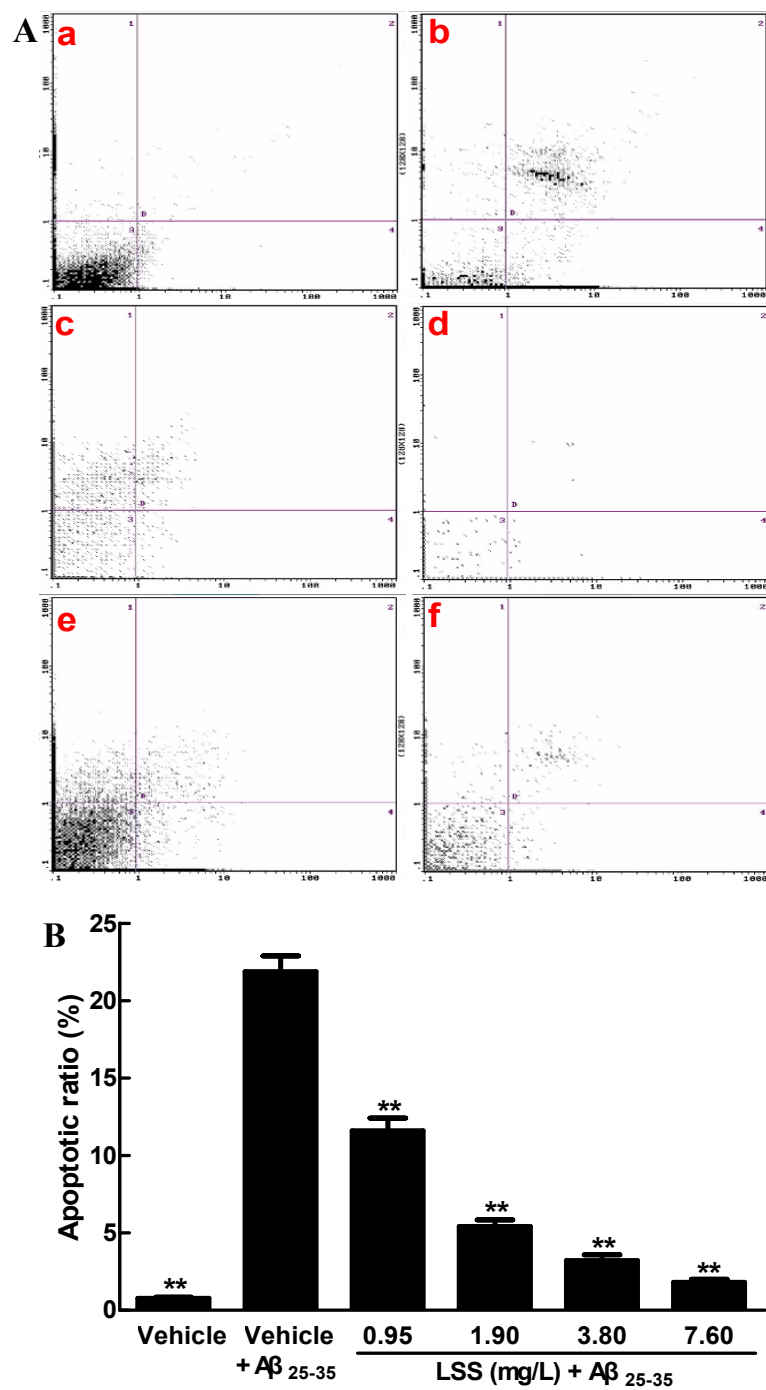
Figure 2. Effect of LSS on apoptosis (**A**) and apoptotic ratio (**B**) induced by $A\beta_{25-35}$ (20 μmol/L) in PC12 cells with Annexin V/PI staining by flow cytometric analysis. (**Aa**) Cells were treated with medium for 13 h without $A\beta_{25-35}$; (**Ab**) cells were treated with medium for 1 h and followed by $A\beta_{25-35}$ for 12 h; (**Ac**) cells were treated with LSS 0.95 mg/L for 1 h and followed by $A\beta_{25-35}$ for 12 h; (**Ad**) cells were treated with LSS 1.90 mg/L for 1 h and followed by $A\beta_{25-35}$ for 12 h; (**Ae**) cells were treated with LSS 3.80 mg/L for 1 h and followed by $A\beta_{25-35}$ for 12 h; (**Af**) cells were treated with LSS 7.60 mg/L for 1 h and followed by $A\beta_{25-35}$ for 12 h; (**B**) Summarized results of apoptotic ratio. The results are representative of at least three independent experiments run in triplicate and expressed as mean $\pm$ SD. ** $p < 0.01$ vs. the cells treated with vehicle and $A\beta_{25-35}$.
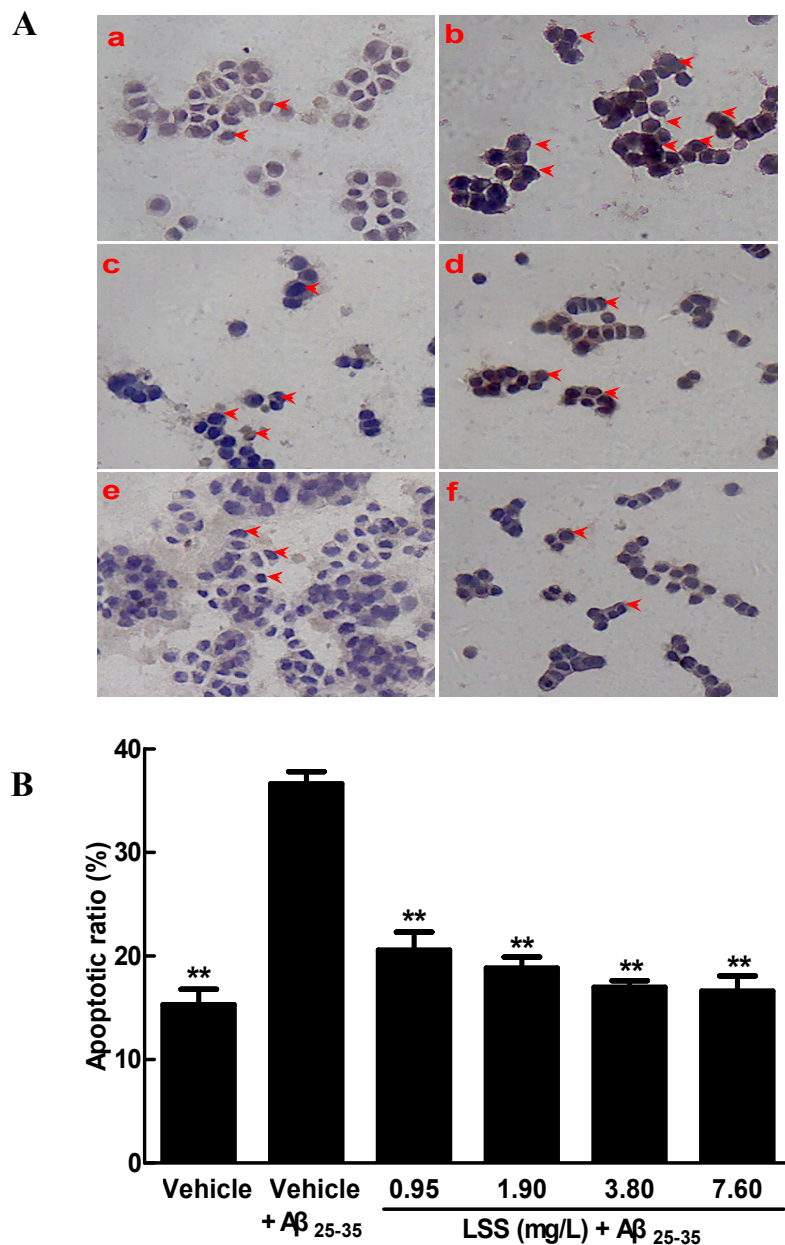
Figure 3. Effect of LSS on apoptosis (**A**) and apoptotic ratio (**B**) induced by $A\beta_{25-35}$ (20 μmol/L) in PC12 cells with TUNEL analysis (×400). (**Aa**) Cells were treated with medium for 13 h without $A\beta_{25-35}$; (**Ab**) cells were treated with medium for 1 h and followed by $A\beta_{25-35}$ for 12 h; (**Ac**) cells were treated with LSS 0.95 mg/L for 1 h and followed by $A\beta_{25-35}$ for 12 h; (**Ad**) cells were treated with LSS 1.90 mg/L for 1 h and followed by $A\beta_{25-35}$ for 12 h; (**Ae**) cells were treated with LSS 3.80 mg/L for 1 h and followed by $A\beta_{25-35}$ for 12 h; (**Af**) cells were treated with LSS 7.60 mg/L for 1 h and followed by $A\beta_{25-35}$ for 12 h. The red arrows indicate apoptotic cells; (**B**) Summarized results of apoptotic ratio. The results are representative of at least three independent experiments run in triplicate and expressed as mean ± SD. ** $p < 0.01$ vs. the cells treated with vehicle and $A\beta_{25-35}$.

3.2. Effect of LSS on Mitochondrial Membrane Potential in PC12 Cells Exposed to Aβ25-35 with Rhodamine 123 Staining

Mitochondria play a key role in the progression of apoptosis. Therefore we examined the effect of LSS on mitochondrial membrane potential in PC12 cells with or without exposure to $A\beta_{25-35}$ (20 μmol/L) for 12 h with rhodamine 123 staining and the results of the representative

photomicrographs are shown in Figure 4. The fluorescence intensity of PC12 cells induced by $A\beta_{25\text{-}35}$ was obviously increased ($p < 0.01$) compared to that of the control cells treated with a medium (Figure 4a,b). However, a significantly decrease in fluorescence intensity was observed after PC12 cells were treated with LSS at 0.95, 1.90 3.80 and 7.60 mg/L for 12 h compared to the control cells treated with medium (Figure 4c–f). The results indicate that the mitochondrial membrane potentials of P12 cells were decreased by LSS compared to vehicle treatment.
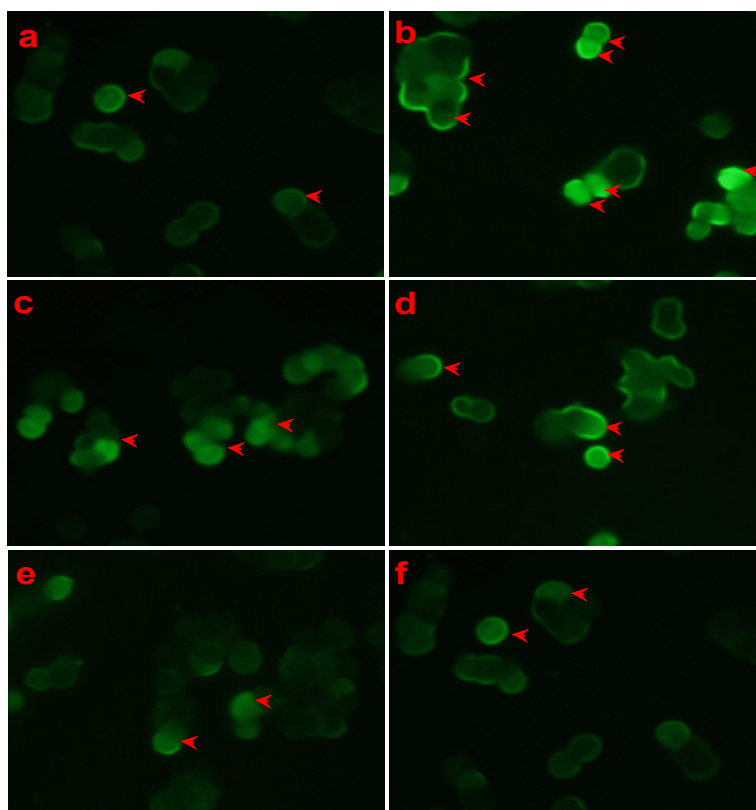

Figure 4. Effect of LSS on mitochondria membrane potential in PC12 cells treated with or without $A\beta_{25\text{-}35}$ (20 μmol/L) with rhodamine 123-staining (400×). (**a**) Cells were treated with medium for 13 h without $A\beta_{25\text{-}35}$; (**b**) cells were treated with medium for 1 h and followed by $A\beta_{25\text{-}35}$ for 12 h; (**c**) cells were treated with LSS 0.95 mg/L for 1 h and followed by $A\beta_{25\text{-}35}$ for 12 h; (**d**) cells were treated with LSS 1.90 mg/L for 1 h and followed by $A\beta_{25\text{-}35}$ for 12 h; (**e**) cells were treated with LSS 3.80 mg/L for 1 h and followed by $A\beta_{25\text{-}35}$ for 12 h; (**f**) cells were treated with LSS 7.60 mg/L for 1 h and followed by $A\beta_{25\text{-}35}$ for 12 h. The red arrows indicate apoptotic cells. The results are representative of at least three independent experiments run in triplicate.

3.3. Effects of LSS on the Protein Expressions of Bcl-2 and Bax in PC12 Cells Induced by $A\beta_{25\text{-}35}$

The protein expressions of Bcl-2 and Bax are crucial for the mitochondria-mediated apoptosis. Therefore, we examined the protein expressions of Bcl-2 and Bax in PC12 cells by Western blotting analysis. The results showed that LSS can inhibit the apoptosis significantly in PC12 cells through regulation the protein expressions of Bcl-2 and Bax. In which the protein expression of Bcl-2 was downregulated, while that of Bax was significantly upregulated exposed to 20 μmol/L $A\beta_{25\text{-}35}$ for 12 h compared to cells treated with a vehicle ($p < 0.01$) (Figure 5A,B). However, LSS at 0.95–7.60 mg/L significantly upregulated the protein expression of *Bcl-2* compared to vehicle treatment ($p < 0.01$) in PC12 cells, which decreased by $A\beta_{25\text{-}35}$ (Figure 5A). Furthermore, LSS also significantly downregulated the overexpression of Bax induced by $A\beta_{25\text{-}35}$ in a concentration-dependent manner compared to vehicle treatment ($p < 0.01$) in PC12 cells (Figure 5B). Therefore, LSS increases the ratio of Bcl-2/Bax in

PC12 cells treated with $A\beta_{25-35}$ in a concentration-dependent manner ($p < 0.01$) (Figure 5C). The results demonstrate that the regulation of the expressions of Bcl-2 and Bax by LSS is an important mechanism of protection of PC12 cells from $A\beta_{25-35}$ induced apoptosis and cell damage.
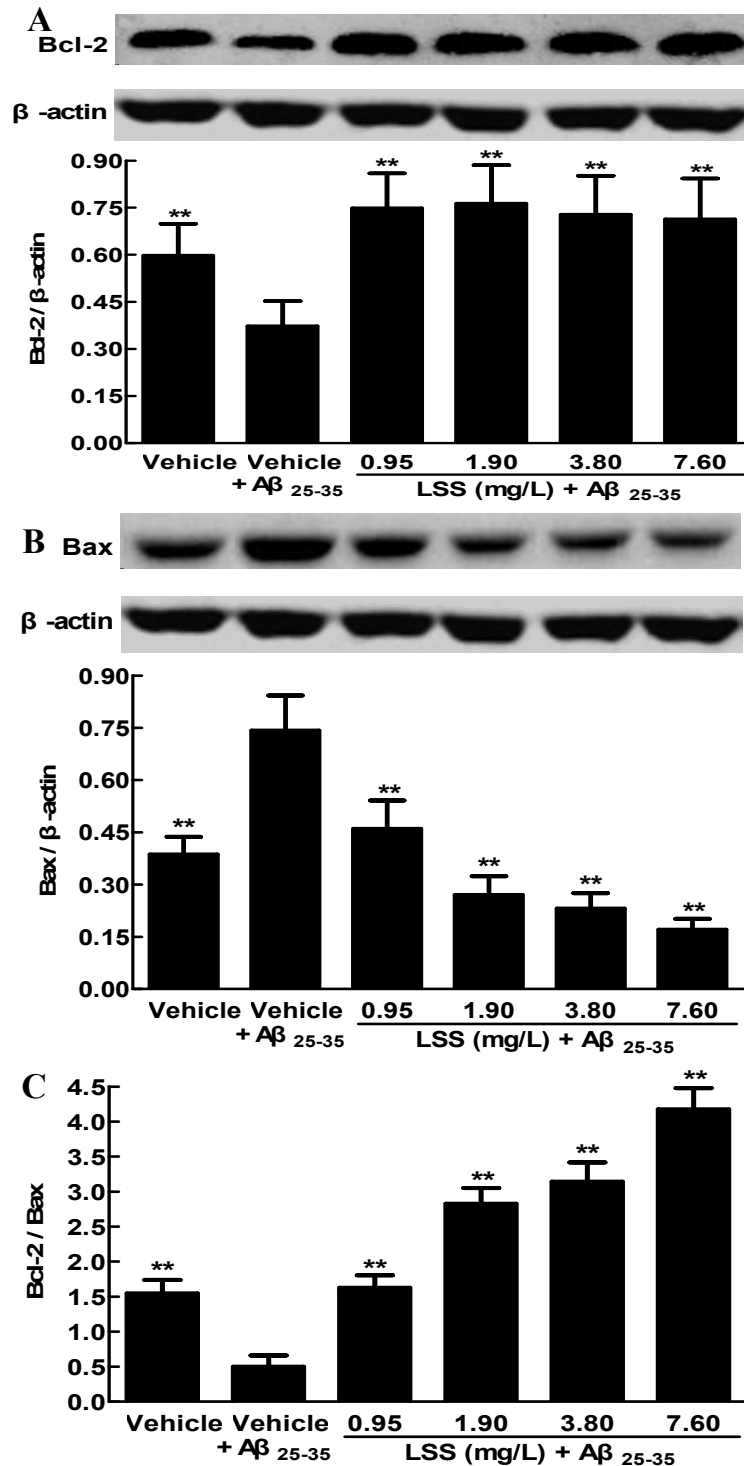
Figure 5. Effects of LSS on the protein expressions of Bcl-2 (**A**), Bax (**B**), and the ratio of Bcl-2/Bax (**C**) in PC12 cells with or without exposure to 20 μmol/L $A\beta_{25-35}$ for 12 h. The results are representative of at least three independent experiments run in triplicate and expressed as mean ± SD. ** $p < 0.01$ vs. the cells treated with $A\beta_{25-35}$ and vehicle.

3.4. Effects of LSS on mRNA Expression and Nuclear Translocation of NF-κBp65 in PC12 Cells Treated with Aβ25-35

We speculated that the effect of LSS on anti-apoptosis may be involved in regulation of the mRNA expression of *NF-κBp65* in PC12 cells. Therefore, the expression levels of *NF-κBp65* and GAPDH were analyzed by RT-PCR in PC12 cells with or without exposure to 20 μmol/L Aβ$_{25-35}$ for 12 h and the results are shown in Figure 6. The data reveal that the mRNA expression of *NF-κBp65* significantly increased in PC12 cells by Aβ$_{25-35}$ compared to the control cells treated with a vehicle ($p < 0.01$). However, LSS (0.95–7.60 mg/L) significantly decreased the mRNA expression of *NF-κBp65* ($p < 0.01$) in a concentration-dependent manner in PC12 cells treated with Aβ$_{25-35}$.
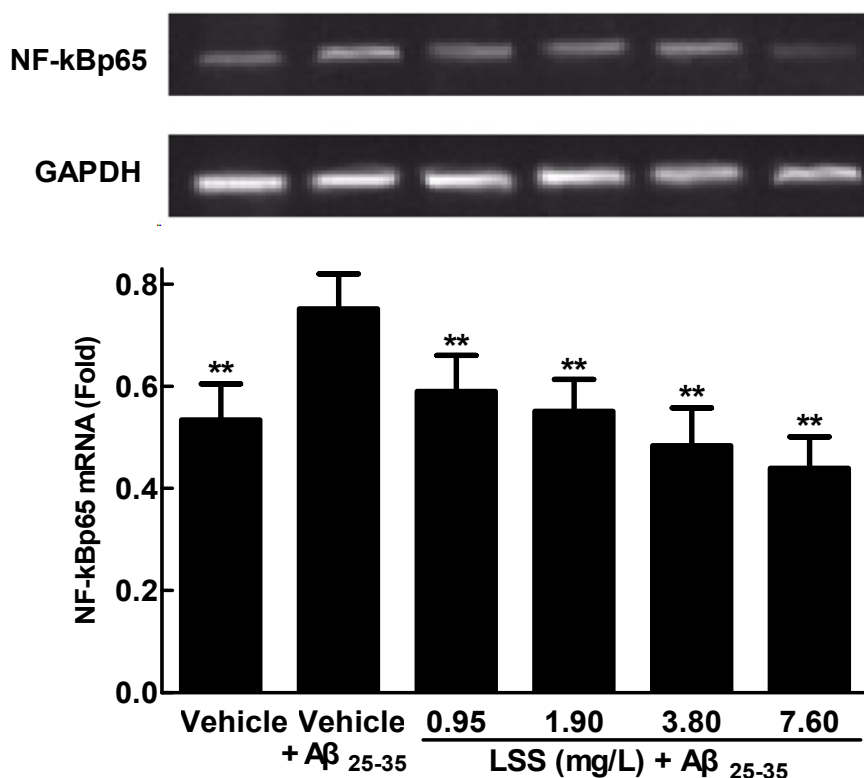
Figure 6. Effect of LSS on the mRNA expression of *NF-κBp65* in PC12 cells treated with Aβ$_{25-35}$ (20 μmol/L). The results are representative of at least three independent experiments run in triplicate and expressed as mean ± SD. ** $p < 0.01$ vs. the cells treated with Aβ$_{25-35}$ and vehicle.

To investigate the effect of LSS on signaling downstream of *NF-κBp65* activation induced by Aβ$_{25-35}$, we further studied the nuclear translocation of *NF-κBp65* in PC12 cells treated with or without 20 μmol/L Aβ$_{25-35}$ by immunofluorescence analysis; and the results are shown in Figure 7. As shown by the representative pictures, *NF-κBp65* was mainly localized in the cytosolic compartment in the control cells treated with vehicle (Figure 7a). While Aβ$_{25-35}$ strongly induced nuclear translocation of *NF-κBp65* (Figure 7b), LSS at 0.95, 1.90, 3.80, and 7.6 mg/L significantly decreased ($p < 0.01$) nuclear translocation of *NF-κBp65* induced by Aβ$_{25-35}$ in a concentration-dependent manner (Figure 7c–f). The results indicate that Aβ$_{25-35}$ markedly elevated mRNA expression and nuclear translocation of *NF-κBp65* and LSS significantly attenuated their increases in PC12 cells.
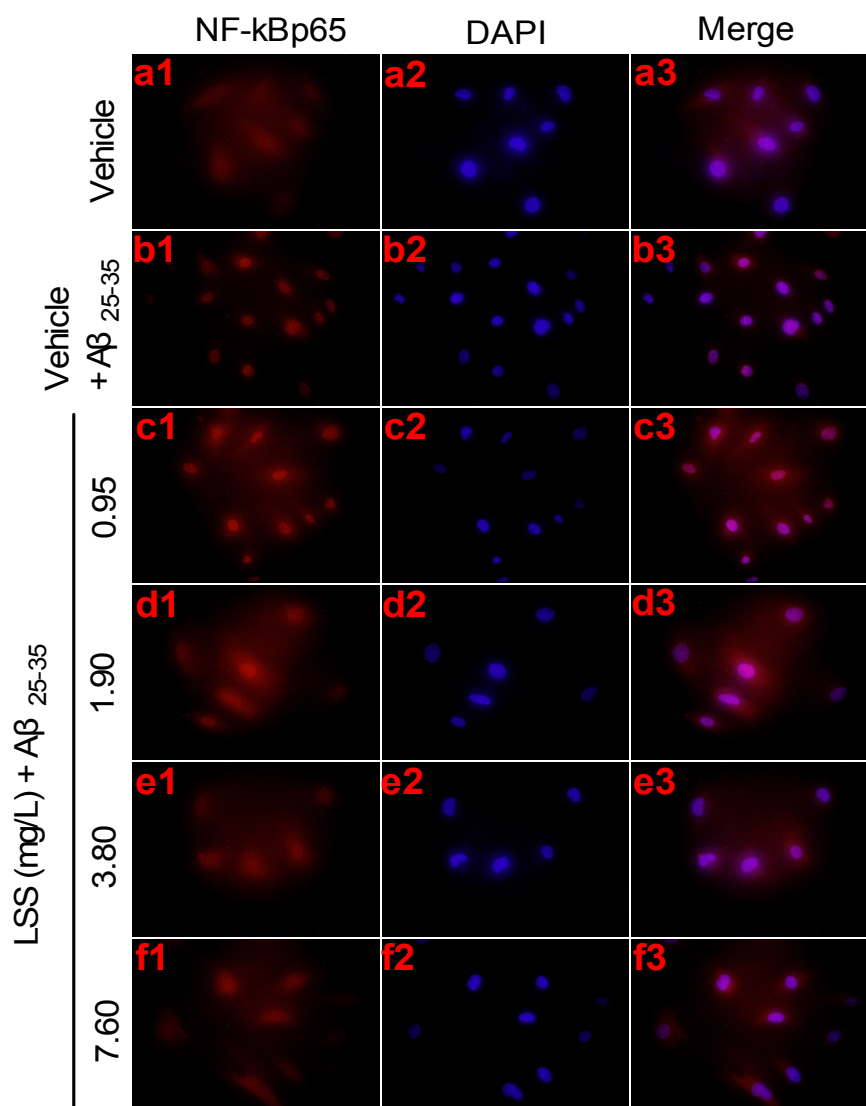
Figure 7. Effect of LSS on nuclear translocation of *NF-κBp65* in PC12 cells treated with or without 20 μmol/L Aβ$_{25-35}$ for 12 h (400×). (**a**) Control cells were treated with medium for 13 h without Aβ$_{25-35}$; (**b**) cells were treated with medium for 1 h and followed by 20 μmol/L Aβ$_{25-35}$ for 12 h; (**c**) cells were treated with LSS 0.95 mg/L for 1 h and following by 20 μmol/L Aβ$_{25-35}$ for 12 h; (**d**) cells were treated with LSS 1.90 mg/L for 1 h and followed by 20 μmol/L Aβ$_{25-35}$ for 12 h; (**e**) cells were treated with LSS 3.80 mg/L for 1 h and followed by 20 μmol/L Aβ$_{25-35}$ for 12 h; (**f**) cells were treated with LSS 7.60 mg/L for 1 h and followed by 20 μmol/L Aβ$_{25-35}$ for 12 h. Numbers preceding letters represent the following: 1. red channel (NF-κB); 2. blue channel (DAPI); and 3. combined figure of red and blue channels. The results are representative of at least three independent experiments run in triplicate.

4. Discussion

The present study aimed to investigate the effects of LSS on apoptosis using three different analysis methods(Hoechst 33342/propidium iodide fluorescence double staining, Annexin V/PI double staining, and terminal deoxynucleotidyl transferase (TdT)-mediated dUTP nick-end labeling), mitochondrial function, protein expressions of *Bcl-2* and *Bax*, and mRNA expression and nuclear translocation of the *NF-κB* signaling pathway-associated apoptotic gene (*p65*) in PC12 cells treated with 20 μmol/L Aβ$_{25-35}$ in vitro. Our results indicate that LSS significantly protects from apoptotic injury to the cells induced by Aβ$_{25-35}$ (Figures 1–3), decreases mitochondria membrane potentials (Figure 4), upregulates the expression of Bcl-2 protein, and downregulates the expressions of *Bax* protein and the

ratio of *Bcl-2/Bax* (Figure 5), and inhibits the mRNA expression and nuclear translocation of *NF-κBp65* (Figures 6 and 7) in Aβ$_{25-35}$-treated PC12 cells. The results suggest that LSS can inhibit Aβ$_{25-35}$-induced apoptosis through improvement of mitochondrial function and suppression of the *NF-κB* signaling pathway. Therefore, our findings suggest that the effect of LSS against AD may be involved with apoptotic and *NF-κB* signaling pathways in PC12 cells.

Aβ, as one of the main toxic peptides and a vital biomarker of neuronal apoptosis for AD, is derived from amyloid-β protein precursor (APP) processing by β-and γ-secretase through the amyloid cascade pathway [29]. Accumulating evidence suggests that Aβ contributes to AD pathogenesis and progress by various mechanisms including DNA fragmentation [30], Tau protein phosphorylation [31], mitochondrial dysfunction [32], and apoptosis induction. Various preclinical studies have provided evidence that Aβ$_{25-35}$ and Aβ$_{1-40}$ can induce neuronal apoptosis in PC12 and SH-SY5Y cells in vitro [33,34] and the hippocampus of brain in rats in vivo [35]. The underlying mechanism involved in neuronal apoptosis may be associated with multiple pathways, including the action of catabolic enzymes [36], release of ROS [36], disruption of mitochondria [37], and activation of the related apoptotic signal pathway and *NF-κB* pathway [38]. Numerous studies have indicated that the mitochondria play a vital role in cellular apoptosis [39,40]. The release of mitochondrial cytochrome c is an early common event in apoptosis [41]. Furthermore, the decrease of mitochondrial membrane potential in cell and apoptosis-related factors are key events in initiating the cascade reaction leading to cell apoptosis [42]. Aβ initiated mitochondrial oxidative stress and increased mitochondrial membrane permeability and cytochrome c release [42] to trigger the caspase cascade [43] and DNA degradation [44], leading to apoptosis. In addition, it is well known that cell survival is initiated by various factors including *NF-κB* and *Akt*, involved with *PI3K/Akt* signal transduction pathway [45]. Classical NF-κB, as a nuclear transcription factor, is a heterodimer composed of *p50/p65* subunits [46]. It is well established that activated forms of *PI3K/Akt* initiated *NF-κB* transcriptional activity, mainly through signaling pathway that stimulated the transactivation domain of the p65 subunit [47].

PC12 cells are derived from adrenal medulla pheochromocytoma in rats and the cells can be induced by some nerve growth factors (NGF) to differentiate into nervous-like cells with similar characteristics to neurons in physiological and/or biochemical aspects [25,48]. The cells with or without NGF are widely used to study various aspects on the field of nervous system in vitro [25,34,49]. In a previous study, we evaluated the cytotoxicity of LSS in PC12 cells to determine the maximum safe concentration and the effective concentration of LSS in protection from Aβ$_{25-35}$ induced cytotoxicity [50,51].

Our previous studies have found that LSS can decrease the formation of Aβ and mitochondrial cytochrome C release, thereby inhibiting neuronal apoptosis in the brain of AD rats [51]. In the present study, we found that the anti-apoptotic effect of LSS in PC12 cells treated with Aβ$_{25-35}$ may be associated with mitochondrial membrane function and the *NF-κB* signaling pathway. The proposed possible mechanisms for LSS effects are summarized in Figure 8. However, it is still unclear whether LSS can affect other signaling pathways such as protein kinase C (*PKC*), *PI3K/Akt*, and *Jak/stat* pathways due to the complexity of the molecular mechanisms in the pathogenesis of AD. Therefore, our further investigation of the molecular mechanisms associated with the effect of LSS on neuronal protection in AD should include the upstream regulation of *PI3K/Akt* and apoptotic pathways, as well as the protein expression and phosphorylation of *P65* and *P50* related to the NF-κB pathway.
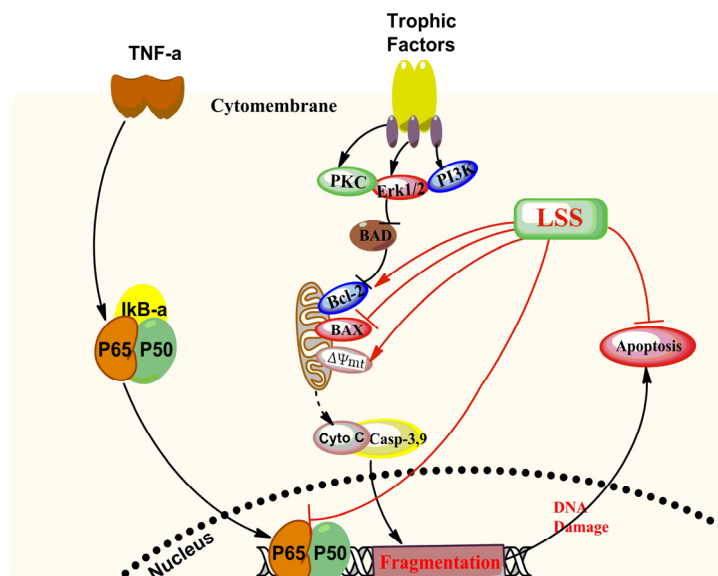
Figure 8. Proposed scheme of possible mechanisms for LSS inhibition of apoptosis induced by $A\beta_{25-35}$ through regulation of the apoptotic and NF-κB pathways in PC12 cells.

5. Conclusions

The present study demonstrated that LSS significantly inhibited apoptosis in PC12 cells induced by $A\beta_{25-35}$. The possible mechanisms may be related to improvement of mitochondrial function via inhibition of the mitochondria membrane permeability, upregulating the expressions of Bcl-2 protein, downregulating the expression of Bax protein, and decreasing the mRNA expression and nuclear translocation of NF-κBp65 in PC12 cells exposed to 20 μmol/L $A\beta_{25-35}$ for 12 h. Therefore, LSS has the potential to be developed as a novel agent or nutrient supplement for the prevention and/or treatment of AD clinically.

Author Contributions: Dalian Qin, Jianming Wu and Xiuling Wang conceived and designed the experiments; Hong Zhang, Xiuling Wang, Jianming Wu, Yong Tang, Rong Chen, Jian Liu, Haixia Chen, Li Gu and Mao Li performed the experiments; Jianming Wu and Dalian Qin analyzed the data; Xiuling Wang, Jianming Wu and Shousong Cao wrote the paper.

Conflicts of Interest: The authors declare no conflict of interest.

References

1. Takata, K.; Takada, T.; Ito, A.; Asai, M.; Tawa, M.; Saito, Y.; Ashihara, E.; Tomimoto, H.; Kitamura, Y.; Shimohama, S. Microglial Amyloid-β_{1-40} phagocytosis dysfunction is caused by high-mobility group box protein-1: Implications for the pathological progression of Alzheimer's disease. *Int. J. Alzheimers Dis.* **2012**, *2012*, 685739. [CrossRef] [PubMed]

2. You, Y.; Yan, L.; Huang, L.Q.; Huang, S.Q.; Zhuang, J.H.; Chen, X.Y.; Lin, Z.; Wu, H.J.; Shao, F.Y.; Zhao, Z.X. Anti-apoptosis effect of astragaloside IV on Alzheimer's disease rat model via enhancing the expression of Bcl-2 and Bcl-xl. *Scand. J. Lab. Anim. Sci.* **2010**, *37*, 75–82.

3. Yadav, R.S.; Tiwari, N.K. Lipid integration in neurodegeneration: An overview of Alzheimer's disease. *Mol. Neurobiol.* **2014**, *50*, 168–176. [CrossRef] [PubMed]

4. Liu, J.; Li, C.; Xing, G.; Zhou, L.; Dong, M.; Geng, Y.; Li, X.; Li, J.; Wang, G.; Zou, D. Beta-asarone attenuates neuronal apoptosis induced by Beta amyloid in rat hippocampus. *Yakugaku Zasshi* **2010**, *130*, 737–746. [CrossRef] [PubMed]

5. Zhang, L.; Li, C.; Quan, R.; Xie, S. The effect of electroacupuncture on neuronal apoptosis and related functions in rats with acute spinal cord injury. *Chin. Med.* **2014**, *5*, 199–210. [CrossRef]

6. Radi, E.; Formichi, P.; Battisti, C.; Federico, A. Apoptosis and oxidative stress in neurodegenerative diseases. *J. Alzheimers Dis.* **2014**, *42*, S125–S152. [PubMed]

7. Kang, D.E.; Roh, S.E.; Woo, J.A.; Liu, T.; Bu, J.H.; Jung, A.R.; Lim, Y. The Interface between cytoskeletal aberrations and mitochondrial dysfunction in Alzheimer's disease and related disorders. *Exp. Neurobiol.* **2011**, *20*, 67–80. [CrossRef] [PubMed]

8. Sharma, V.; Thakur, V.; Singh, S.N.; Guleria, R. Tumor necrosis factor and Alzheimer's disease: A cause and consequence relationship. *Klin. Psikofarmakol. Bul.* **2012**, *22*, 86–97. [CrossRef]

9. Mei, J.M.; Niu, C.S. Effects of CDNF on 6-OHDA-induced apoptosis in PC12 cells *via* modulation of Bcl-2/Bax and caspase-3 activation. *Neurol. Sci.* **2014**, *35*, 1275–1280. [PubMed]

10. Zhang, H.; Wu, S.; Xing, D. Inhibition of $A\beta_{25\text{-}35}$-induced cell apoptosis by Low-power-laser-irradiation (LPLI) through promoting Akt-dependent YAP cytoplasmic translocation. *Cell Signal.* **2012**, *24*, 224–232. [CrossRef] [PubMed]

11. Ali, T.; Kim, M.O. Melatonin ameliorates amyloid beta-induced memory deficits, tau hyperphosphorylation and neurodegeneration *via* PI_3/Akt/GSk3β pathway in the mouse hippocampus. *J. Pineal. Res.* **2015**, *59*, 47–59. [CrossRef] [PubMed]

12. Inoue, M.; Fujishiro, N.; Imanaga, I.; Sakamoto, Y. Role of ATP decrease in secretion induced by mitochondrial dysfunction in guinea-pig adrenal chromaffin cells. *J. Physiol.* **2002**, *539*, 145–155. [CrossRef] [PubMed]

13. Marsillach, J.; Ferré, N.; Camps, J.; Riu, F.; Rull, A.; Joven, J. Moderately high folic acid supplementation exacerbates experimentally induced liver fibrosis in rats. *Exp. Biol. Med.* **2008**, *233*, 38–47. [CrossRef] [PubMed]

14. Obulesu, M.; Lakshmi, M.J. Apoptosis in Alzheimer's disease: An understanding of the physiology, pathology and therapeutic avenues. *Neurochem. Res.* **2014**, *39*, 2301–2312. [CrossRef] [PubMed]

15. Zhang, J.; Zhang, C. Research progress on the antineoplastic pharmacological effects and mechanisms of litchi seeds. *Chin. Med.* **2015**, *6*, 20–26. [CrossRef]

16. Prasad, K.N.; Yang, B.; Yang, S.; Chen, Y.; Zhao, M.; Ashraf, M.; Jiang, Y. Identification of phenolic compounds and appraisal of antioxidant and antityrosinase activities from litchi (*Litchi sinensis* Sonn.) seeds. *Food Chem.* **2009**, *116*, 1–7. [CrossRef]

17. Xu, X.; Xie, H.; Wang, Y.; Wei, X. A-type proanthocyanidins from lychee seeds and their antioxidant and antiviral activities. *J. Agric. Food Chem.* **2010**, *58*, 11667–11672. [CrossRef] [PubMed]

18. Wei, L.I.; Zhu, Y.T.; Huang, Z.Y.; He, J.J.; Pei, J. Experimental studies on anti-fluvirus effect of litchi seed in vivo. *Chin. J. Ethnomed. Ethnopharm.* **2011**, *9*, 34–36.

19. Xiao, L.; Pan, J.; Rao, W. The research of protective effect of litchi seed of experimental liver injury in mice. *China J. Tradit. Chin. Med. Pharm.* **2005**, *20*, 42–43.

20. Deng, Z.J.; Guo, J.W.; Pan, J.Q. Pharmacologic and pharmacodynamic effects of effective element of litchi and litchi seed. *Pharma. Today* **2009**, *19*, 7–9.

21. Xiao, Z.; Guo, J.; Feng, X.U.; Pharmacy, D.O.; Hospital, F.C. Effect of litchi saponin and litchi flavones on insulin resistance in $HepG_2$ cells. *J. Pharma. Pract.* **2015**, *33*, 316–318.

22. Yaidikar, L.; Thakur, S. Arjunolic acid, a pentacyclic triterpenoidal saponin of Terminalia Arjuna bark protects neurons from oxidative stress associated damage in focal cerebral ischemia and reperfusion. *Pharmacol. Rep.* **2015**, *67*, 890–895. [CrossRef] [PubMed]

23. Liu, J.F.; Yan, X.D.; Qi, L.S.; Li, L.; Hu, G.Y.; Li, P.; Zhao, G. Ginsenoside Rd attenuates $Abeta_{25\text{-}35}$-induced oxidative stress and apoptosis in primary cultured hippocampal neurons. *Chem. Biol. Interact.* **2015**, *239*, 12–18. [CrossRef] [PubMed]

24. Wan, Q. The intervention of Lychee seed saponins on rats with Alzheimer's disease. *Luzhou Med. Coll.* **2010**, *33*, 1–3.

25. Qian, X.; Cao, H.; Ma, Q.; Wang, Q.; He, W.; Qin, P.; Ji, B.; Yuan, K.; Yang, F.; Liu, X. Allopregnanolone attenuates $A\beta_{25\text{-}35}$-induced neurotoxicity in PC12 cells by reducing oxidative stress. *Int. J. Clin. Exp. Med.* **2015**, *8*, 13610–13615. [PubMed]

26. Hu, Z.; Guan, W.; Wang, W.; Huang, L.; Xing, H.; Zhu, Z. Synthesis of b-alanine C60 derivative and its protective effect on hydrogen peroxide-induced apoptosis in rat pheochromocytoma cells. *Cell Biol. Int.* **2007**, *31*, 798–804. [PubMed]

27. Schutte, B.; Nuydens, R.; Geerts, H.; Ramaekers, F. Annexin V binding assay as a tool to measure apoptosis indifferentiated neuronal cells. *J. Neurosci. Meth.* **1998**, *86*, 63–69. [CrossRef]

28. Jang, J.H.; Aruoma, O.I.; Jen, L.S.; Chung, H.Y.; Surh, Y.J. Ergothioneine rescues PC12 cells from β-amyloid-induced apoptotic death. *Free Radic. Biol. Med.* **2004**, *36*, 288–299. [CrossRef] [PubMed]

29. Myhre, O.; Utkilen, H. Metal dyshomeostasis and inflammation in Alzheimer's and Parkinson's diseases: Possible impact of environmental exposures. *Oxid. Med. Cell. Longev.* **2013**, *2013*, 726954. [PubMed]

30. Yagami, T.; Ueda, K.; Sakaeda, T.; Itoh, N.; Sakaguchi, G.; Okamura, N.; Hori, Y.; Fujimoto, M. Protective effects of a selective L-type voltage-sensitive calcium channel blocker, S-312-d, on neuronal cell death. *Biochem. Pharmacol.* **2004**, *67*, 1153–1165. [CrossRef] [PubMed]

31. Resende, R.; Ferreiro, E.; Pereira, C.; Oliveira, C.R. ER stress is involved in Aβ-induced GSK-3β activation and tau phosphorylation. *J. Neurosci. Res.* **2008**, *86*, 2091–2099. [CrossRef] [PubMed]

32. Ye, C.Y.; Lei, Y.; Tang, X.C.; Zhang, H.Y. Donepezil attenuates Aβ-associated mitochondrial dysfunction and reduces mitochondrial Aβ accumulation in vivo and in vitro. *Neuropharmacology* **2015**, *95*, 29–36. [CrossRef] [PubMed]

33. Chang, W.; Teng, J. β-asarone prevents Aβ$_{25-35}$-induced inflammatory responses and autophagy in SH-SY5Y cells: Down expression Beclin-1, LC3B and up expression Bcl-2. *Int. J. Clin. Exp. Med.* **2015**, *8*, 20658–20663. [PubMed]

34. Xu, J.; Zhang, R.; Zuo, P.; Yang, N.; Ji, C.; Liu, W.; Wang, Y.; Wang, H.; Wu, A.; Yue, Y. Aggravation effect of isoflurane on Aβ$_{(25-35)}$-induced apoptosis and tau hyperphosphorylation in PC12 cells. *Cell Mol. Neurobiol.* **2012**, *32*, 1343–1351. [PubMed]

35. Tian, X.Q.; Zhang, L.D.; Wang, J.M.; Dai, J.G.; Shen, S.S.; Yang, L.; Huang, P.L. The protective effect of hyperbaric oxygen and *Ginkgo biloba* extract on Aβ$_{25-35}$-induced oxidative stress and neuronal apoptosis in rats. *Behav. Brain Res.* **2013**, *242*, 1–8. [CrossRef] [PubMed]

36. Jazvinšćak, J.M.; Hof, P.R.; Šimić, G. Ceramides in Alzheimer's disease: Key Mediators of Neuronal Apoptosis Induced by Oxidative Stress and Aβ Accumulation. *Oxid. Med. Cell. Longev.* **2015**, *2015*, 1–17. [CrossRef] [PubMed]

37. Cavallucci, V.; Ferraina, C.; D'Amelio, M. Key role of mitochondria in Alzheimer's disease synaptic dysfunction. *Curr. Pharm. Des.* **2013**, *19*, 6440–6450. [CrossRef] [PubMed]

38. Yu, Y.; Zhou, L.; Sun, M.; Zhou, T.; Zhong, K.; Wang, H.; Liu, Y.; Liu, X.; Xiao, R.; Ge, J. Xylocoside G reduces amyloid-β induced neurotoxicity by inhibiting NF-κB signaling pathway in neuronal cells. *J. Alzheimers Dis.* **2012**, *30*, 263–275. [PubMed]

39. Schmitt, K.; Brown, S.; Frank, S.; Eckert, A. Mitochondrial dynamics in Alzheimer's disease. *Drug Aging* **2010**, *27*, 181–192. [CrossRef]

40. Morais, V.A.; De, S.B. Mitochondria dysfunction and neurodegenerative disorders: Cause or consequence. *J. Alzheimers Dis.* **2010**, *20*, S255–S263. [PubMed]

41. Kadenbach, B.; Arnold, S.; Lee, I.; Hüttemann, M. The possible role of cytochrome c oxidase in stress-induced apoptosis and degenerative diseases. *Biochim. Biophys. Acta* **2004**, *1655*, 400–408. [PubMed]

42. Bartley, M.G.; Marquardt, K.; Kirchhof, D.; Wilkins, H.M.; Patterson, D.; Linseman, D.A. Overexpression of amyloid-β protein precursor induces mitochondrial oxidative stress and activates the intrinsic apoptotic cascade. *J. Alzheimers Dis.* **2012**, *28*, 855–868. [PubMed]

43. Yu, W.; Mechawar, N.; Krantic, S.; Quirion, R. Evidence for the involvement of apoptosis-inducing factor–mediated caspase-independent neuronal death in Alzheimer disease. *Am. J. Pathol.* **2010**, *176*, 2209–2218. [CrossRef] [PubMed]

44. Gao, J.; Inagaki, Y.; Liu, Y. Research progress on flavonoids isolated from traditional Chinese medicine in treatment of Alzheimer's disease. *Intract. Rare Dis. Res.* **2013**, *2*, 3–10.

45. Gong, Q.H.; Shi, X.R.; Hong, Z.Y.; Pan, L.L.; Liu, X.H.; Zhu, Y.Z. A new hope for neurodegeneration: Possible role of hydrogen sulfide. *J. Alzheimers Dis.* **2011**, *24*, 173–182. [PubMed]

46. Singh, B.N.; Shankar, S.; Srivastava, R.K. Green tea catechin, epigallocatechin-3-gallate (EGCG): Mechanisms, perspectives and clinical applications. *Biochem. Pharmacol.* **2011**, *82*, 1807–1821. [CrossRef] [PubMed]

47. Basnet, P.; Skalko-Basnet, N. Curcumin: An anti-inflammatory molecule from a curry spice on the path to cancer treatment. *Molecules* **2011**, *16*, 4567–4598. [CrossRef] [PubMed]

48. Puangmalai, N.; Somani, A.; Thangnipon, W.; Ballard, C.; Broadstock, M. A genetically immortalized human stem cell line: A promising new tool for Alzheimer's disease therapy. *EXCLI J.* **2015**, *14*, 1135–1144. [PubMed]

49. Li, N.; Liu, B.; Dluzen, D.E.; Jin, Y. Protective effects of ginsenoside Rg2 against glutamate-induced neurotoxicity in PC12 cells. *J. Ethnopharmacol.* **2007**, *111*, 458–463. [CrossRef] [PubMed]

50. Qin, D.; Zhang, H.; Liu, J.; Zhang, Z.; Wang, L.; Yin, H. Cytotoxicity of Lychee seed saponins on normal PC12 cell and determination of their effective concentration to inhibit cytotoxicity of Aβ. *J. Luzhou Med. Coll.* **2011**, *34*, 594–598.

51. Wang, X.; Wu, J.; Yu, C.; Tang, Y.; Liu, J.; Chen, H.; Jin, B.; Mei, Q.; Cao, S.; Qin, D. Lychee seed saponins improve cognitive function and prevent neuronal injury via inhibiting neuronal apoptosis in a rat model of Alzheimer's disease. *Nutrients* **2017**, *9*, 105. [CrossRef] [PubMed]